

Studies on Curie Temperature in Relation to the Magnetic and Electrical Properties Zn & Sb substituted Cu Ferrites

R.Dhanaraju^a, M.KRaju^a, V.Brahmajirao^b, S.Bangarraju^a

^aMaterial Science Research Laboratories & Central Instrumentation Facility, Department of Physics, Andhra University, Visakhapatnam-530005., INDIA

^bMatrix Institute of Technology, Jawaharlal Nehru Technological University, HYDERABAD-500072, INDIA .
Dept. of Nano science and Technology, School of Biotechnology, MGNIRSA, D.Swaminathan Research Foundation, [DSRF] Gaganmahal, HYDERABAD-500015, INDIA

ABSTRACT

This paper reports about our Synthesis using solid solution Ceramic method & Curie temperature and related Magnetic and other supporting experimental studies on Two series of doped Spinel ferrites (a) $Cu_{(1-x)}Zn_xFe_2O_4$ (b) $Cu_{(1-x)}Sb_xFe_2O_4$ Where, x varies from($x = 0.0 - 1.0$) in steps of 0.2. Our results are presented as plots between (1) dopant concentration and Curie temperature and (2) frequency versus initial permeability. Coercivity measurements and correlation with microstructure and morphology analysis, point out concurrent conclusions with many findings of several authors cited from literature.

Keywords: *Doped Spinel Ferrites, Curie temperature, Coercivity, VSM magnetic studies, Pendulum Magnetometer Technique, Permeability, Verwey's Hopping Transition, Neel's temperature, Super Para magnetism, exchange interactions*

1. INTRODUCTION

Magnetism can be classified broadly into five categories. They are diamagnetic, paramagnetic, ferromagnetic, antiferromagnetic and ferri magnetic. Nano sized magnetic particles have properties, which are drastically different from those of the corresponding bulk materials. Ferrites are ferri magnetic materials and they can be further classified into three, based on their crystal structure.[1] They are spinels, with cubic crystal structure, garnets, with cubic crystal structure and magnetoplumbites, with hexagonal crystal structure.

Spinel ferrites resemble the structure of the naturally occurring mineral ($MgAl_2O_4$). The spinel ferrites have the general formula $\{(M)_{\delta}(Fe)_{(1-\delta)}\}[(M)_{(1-\delta)}(Fe)_{(1+\delta)}]O_4$. The divalent metal ion M (eg:- Zn, Mg, Mn, Fe, Co, Ni or a mixture of them) can occupy either tetrahedral(A) or octahedral(B) sites. In the above formula when ($\delta = 1$), it is called a normal spinel. ($ZnFe_2O_4$, and ($CdFe_2O_4$), are examples of normal ferrites. They exhibit net magnetization at room temperature. The reason for this anomalous Behavior of Nano zinc ferrites is still unknown and many schools of thought exist. When ($\delta = 0$), it is called an inverse spinel and examples are $NiFe_2O_4$, $CoFe_2O_4$, $CuFe_2O_4$ etc. When ($\delta = 1/3$), it is called a random spinel. The origin of the magnetic properties of ferrites arises from the spin magnetic moment of the unpaired transition metal 3d electrons coupled by the

super exchange interaction via the oxygen separating them [2]. It has long been known that the A-O-B exchange interaction is much stronger than the B-O-B and the A-O-A interactions [3,4,& 5to7]. The systems where one or both the sub lattices are populated with magnetic ions, the competing exchange interactions may lead to topological frustration, yielding a magnetic structure that may include states of antiferromagnetic order, local spin canting, spin glass behavior, disordered phases and ferrimagnetic order. Experimental studies on spinel ferrites have shown that they are replete with this rich variety of magnetic ordering that ranges from classical ferrimagnetic ordering to spin Glass behavior [2].

2. EXPERIMENTAL METHODS AND MATERIALS AND TECHNIQUES

2.1 Materials and synthesis

Two series of Doped ferrites *i.e.*, (1) $Cu_{(1-x)}Zn_xFe_2O_4$ (2) $Cu_{(1-x)}Sb_xFe_2O_4$

Where, x varies from $x = (0.0$ to $1.0)$ in steps of 0.2 are synthesized by the solid state ceramic method, using Nabertherm Furnace with Eurotherm controller. The details of the method used in our laboratories and the details of characterization techniques etc., are available elsewhere [9to 11]

2.2 Characterization of Material

Before studying different properties of ferrites, these are characterized by XRD and Curie temperature measurement techniques. The properties of the basic ferrite ($\text{Cu}_{(1-x)}\text{Zn}_x\text{Fe}_2\text{O}_4$) and ($\text{Cu}_{(1-x)}\text{Sb}_x\text{Fe}_2\text{O}_4$) has been put to the following measurements for characterization.

- Lattice constant obtained by the x-ray diffraction studies. The details of the evaluation were reported elsewhere [11,12]
- Curie temperature of the material. The below Table 1 gives the comparison of the values

TABLE 1: Lattice constant AND Curie temperature data for undoped CuFe_2O_4

Parameter	Observed value in our experiments	Reported value in literature
Lattice constant (Å°)	8.3845	8.3970
Curie Temperature (T_c) in $^\circ\text{K}$	552	558

2.3 Magnetization Studies

Thermo magnetization studies were carried out in the temperature range 80-300 K, on these samples of doped zinc ferrites by employing The *Pendulum Magnetometer Technique* (shown in Fig 1 (b)) at Material science Research Laboratories ,Dept. of Physics ,Andhra university , Visakhapatnam-530003, A.P. India & *Vibrating Sample Magnetometer, ("LAKE SHORE" Model 7404)*, that can perform magnetic measurements for materials research and development , at the C.I.L. Hyderabad Central University, Gachibowli, Hyderabad-500046, A.P., (India). Photos (a) , (b), (c) and (d), shown in Fig 1 below depict the system, the locations of the pickup coils , and suspension, and close up view of the magnet set up. Measurement of moments as small as 0.1×10^{-6} emu in magnetic fields ranging from -18 to $+18$ kG is possible with this *VSM System*. Bipolar power supply provides smooth continuous transition through zero fields in it. Initial permeability at room temperature was measured as a function of substituent concentration (x) and frequency. The results are presented as two types of plots (a) between dopant concentration versus Curie temperature, and (b) Frequency versus Initial permeability.

2.4 Vibrating Sample Magnetometer

The vibrating sample magnetometer (VSM) was invented by Simon Foner [13]. The magnetic moment of the sample is detected by pickup coils near the vibrating sample in an adjustable applied magnetic field. The field may be produced by an electromagnet, superconducting magnet, or Bitter magnet. A system using an electromagnet is shown. The VSM is extremely sensitive, suitable for small or weakly magnetic samples, either solid or powder. It is the primary test method for powders. The temperature may be varied from absolute zero to well above the Curie temperature, with little difficulty. The moment is usually calibrated with a Ni standard, taking $4\pi M_s = 6115$ Gauss at 10^4 , Oe and 20°C . [14.15]

2.5 Curie temperature and Experimental setup for its measurement

The Curie temperature (T_c) is nothing but the transition temperature at which the ferromagnetic state of the material changes to paramagnetic state. In ferromagnetic materials the alignment of magnetic moments in a magnetic field at higher temperature is decreased. With further temperature increase, the thermal agitation will exceed the exchange forces and at a certain temperature called the Curie Point,[16] ferromagnetism disappears. Above the Curie point, the ferromagnetic material becomes paramagnetic, the susceptibility of which decreases with temperature. If the reciprocal susceptibility, $(1/\chi)$ is plotted against T, the curve obeys the Curie Weiss Law; $[1/\chi] = \{1/C(T - T_c)\}$, Where C

is Curie Weiss constant and T_c is Curie temperature. In ferromagnetism, the interaction of atomic spin moments was a positive one meaning that the exchange interaction aligned neighboring spins parallel in a magnetic domain. In his study of the paramagnetic susceptibility of certain alloys, Neel [17] noticed that they did not follow the Curie law at low temperatures but did obey the Curie-Weiss law at high temperatures;

$$\chi = C/(T + \theta), \quad \text{Where } \theta \text{ is experimentally determined constant?}$$

Also he found that: $\chi = C/(T - T_N)$, Where T_N is Neel Temperature .This was explained by postulating a negative exchange interaction aligning the neighboring spins antiparallel. The different techniques that were employed for the measurement of Curie temperature in the investigations are cited below.

2.6 Curie temperature by Differential Scanning Calorimeter Technique (DSC TECHNIQUE) - for Phase transitions

This method is used to determine temperatures, by estimating the heat flow, & thermal conductivity, associated with phase transitions in the material. *Modulated DSC 2910 model* was used to determine Curie temperature. The heat capacity and Thermal conductivity were measured. Rath et al [18] also adopted this method to study the polycrystalline material. Our observations, evaluations and the analysis with the DSC Technique are incomplete and are in progress for the specimens and would be published soon.

2.6 Curie Temperature by Pendulum Magnetometer Technique

We determined Curie temperature using the Pendulum magnetometer technique developed by Rathenau and Snoek [19, 20] which employs the principle of transition of the material from the ferromagnetic state changes to paramagnetic state, just at the Curie temperature. The typical set up is shown below. In this method, a small piece of ferrite sample is attached to the lower end of an iron rod and the upper end of which is placed vertically in contact with a pole piece of permanent electromagnet. The lower end of the iron rod along with the sample was enclosed in a furnace having a thermocouple for monitoring temperature. The temperature of the furnace is gradually increased till the ferrite sample loses its magnetization, falls due to gravity. The temperature at which the sample falls is taken as T_c . In this method, a small piece of ferrite sample is attached to the lower end of an iron rod and the upper end of which is placed vertically in contact with a pole piece of permanent electromagnet. The lower end of the iron rod along with the sample was enclosed in a furnace having a thermocouple for monitoring temperature. The temperature of the furnace is gradually increased till the ferrite sample loses its magnetization, falls due to gravity. The temperature at which the sample falls is taken as T_c . However this method is getting replaced by better methods.

2.7 Initial Permeability

Initial permeability may be considered as a measure of efficiency of magnetic material in electrical and magnetic allied applications. It is dependent on many parameters such as stoichiometry, grain structure, composition, impurity content, crystal anisotropy and porosity, like all properties of ferrite materials depend on the preparation and hence on above parameters.

2.8 Measurement of Frequency dependence of Initial Permeability

In our laboratories Initial permeability (μ_i) measurements at room temperature were done on toroid samples at a frequency of 10 kHz. For this purpose, **Hewlett Packard 4192 – impedance analyzer** was utilized by us. Since the ferrite materials contain pores, the initial permeability values are corrected ($(\mu_i - 1)_c$ to micro density ($d_{x\text{-ray}}$ density) in order to eliminate the effects of pores between the grains on the μ_i values by using the following relation [21]. $(\mu_i - 1)_c = \{(\mu_i - 1) d_{x\text{-ray}}\} / d_{\text{Bulk}}$, Where $(\mu_i - 1)_c$ is the corrected initial permeability, and d_{Bulk} is the observed density. Variation of initial permeability of the ferrite materials with frequency in different ranges was determined by measuring inductance of the material adopted by I.C.Beck [22]. Ferrite samples in the form of toroid of outer diameter 1.49 cm were used. The 30 SWG enameled copper wire with 30 turns winding was used on these toroids. The inductance (L) was measured with the HP impedance analyzer-4192, (5Hz to 13 MHz) coupled with a standard signal generator. The details of impedance analyzer setup that was used are available elsewhere [56]. The Permeability is calculated using the formula: $[\mu = L/L_0]$

$$\text{Where } L_0 = 4.6 N^2 \log \left(\frac{OD}{ID} \right) t \times 10^{-9},$$

Henry is the air core inductance, OD = Outer diameter, N = No of turns, ID = Inner diameter and t = thickness of the sample.

Initial permeability at room temperature was measured as a function of substituent concentration (x) and frequency.

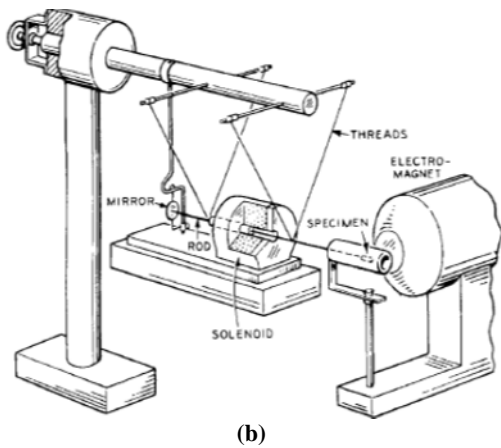
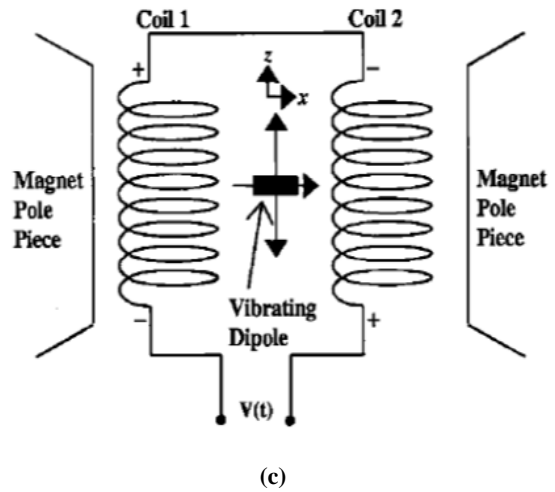
3. RESULTS AND DISCUSSION

In contrast to bulk compound, the Nano crystalline $ZnFe_2O_4$ system always shows up as a mixed spinel in which Zn^{2+} and Fe^{3+} ions are distributed over the A and B-sites. This cationic rearrangement leads to the formation of two magnetic sub lattices, which is responsible for the enhanced magnetization displayed when compared with normal $ZnFe_2O_4$, [23to25]. It is known that the bulk $ZnFe_2O_4$ is a paramagnet at room temperature, however, magnetic order has been observed in its nanoparticles at room temperature [26to32], and similar reports of magnetic.

Properties in $ZnFe_2O_4$ ferrite thin films [33to37]. Yan Xu [38] reported the morphology, structure, and Magnetic properties of $ZnFe_2O_4$ Nanotubes, & their dependence on temperature and concluded that the samples exhibit typical super Para magnetism at room temperature. They concluded that the samples are indeed the mixed spinels

with the Curie temperature at least higher than the observed blocking temperature. Below the blocking temperature, the ZnFe_2O_4 nanotubes are in the ferromagnetic state, and above the blocking temperature nanotubes are at the super paramagnetic state. Their Hysteresis plots point out that at 150 K, the coercivity is near to zero, which shows that the sample is completely super paramagnetic. Most of our observations in the hysteresis studies with our samples show marked similarity with these findings [39].

Fig 1: (a) "LAKE SHORE" VSM (Model 7404) Setup at Hyderabad Central University, A.P.,INDIA, (Manufactured by Lake Shore Cryotronics, 575 McCorkle Blvd, Westerville, Ohio 43082, USA) and (b) the sketch of Typical Pendulum Magnetometer Technique (basic model developed by Rathenau.& Snoek), used in Mat. Sci. Research. Labs, Andhra University, Visakhapatnam. A.P.(INDIA), (c) Sketch giving the locations of vibrating dipole, pickup coils and suspension between the pole pieces of the electromagnet of the VSM System. (d) The Magnet and the suspension assembly of the VSM system.



S.R. Sawant et.al., [40], found that Magnetization for both slow cooled and quenched samples of $\text{Cu}_x\text{Zn}_{1-x}\text{Fe}_2\text{O}_4$ as a function of Zn content has shown a maximum at ($x = 0.6$) and a decrease for ($x > 0.6$). The increase of magnetization is explained on the basis of Neel's two sub-lattice models while the decrease of magnetization is explained on a three sub-lattice model where Quenched samples showed higher magnetization than the slow cooled ones and this increased with the increase of temperature of quenching. The cation transfer between the two sites, characteristic of the temperature that can be frozen-in seems to govern this. Variation of (M_r/M_s) with the content of Zn for both slow cooled and quenched samples indicated more impedance to the domain wall motion or higher Zn content. As the temperature of quenching is increased (M_r/M_s) decreases and this is attributed to detect cluster formation.

H. Ehrhardt, et.al.[41], S. Bid et.al.,[42],and A. Kundu, et.al.,[43],in their studies(including the microstructure characterization by Rietveld’s analysis) on normal and partially inverted zinc ferrite synthesized by different techniques point out similar conclusions ,supporting our findings.

3.1 Our Findings

The results are presented as two types of plots (a) between dopant concentration versus curie temperature, and (b) Frequency versus Initial permeability. The observed fall in Curie temperature (T_c) with increasing concentration of Zinc/ Antimony is shown in Fig. 5.2. The T_c of these samples has been obtained from the differential scanning calorimeter results in which plots are drawn between temperature and heat capacity (H_C). Initially, the rise of H_C with temperature is found to show rapid increase and relatively more sharply up to reaching T_c for low concentrations of Zn^{2+} than Sb^{5+} . Beyond T_c the H_C decreases with temperature. The T_c is found to decrease continuously for both the substituents. This behavior could be attributed in the following manner.

The variation of Curie temperature (T_c) is explained on the basis of AA, BB and AB interactions. The decrease in AB interactions due to A and B sites occupancy of cations decreases the overlap of orbitals, which in turn weaken

the exchange and change the lattice constant [44]. The substituents Sb^{5+} are diamagnetic and these additions either A site or B site weaken the A-B interaction and lowers Curie temperature [17, 45]. According to Neel’s molecular field theory [46], A-B exchange interaction is stronger than A-A or B-B exchange interactions. The exchange interactions between the magnetic ions in A and B lattices increase with both the number and magnetic moment of the magnetic ions at A and B sites. Thus, greater amount of thermal energy will be required to offset the effects of exchange interaction in case of materials having large number of magnetic ions and larger magnetic moments at A and B sites. Replacement of a Fe^{3+} magnetic ion at A and B sites of the crystal structure by diamagnetic ions will results in the reduction of the number of magnetic linkage and consequently in fall of Curie temperature [48 to 50]. Decrease of T_c with substituent concentration (x) in this study is similarly observed.

3.2 Relationship between μ_i and D_g

Initial permeability (μ_i) and grain size (D_g) are two important parameters to evaluate quality and behavior of a ferrite. During recent years non-magnetic grain boundary (NMGB) model [51] is given due importance over Globus model. However, for larger grains Globus model could be adopted to understand microstructure of the material.

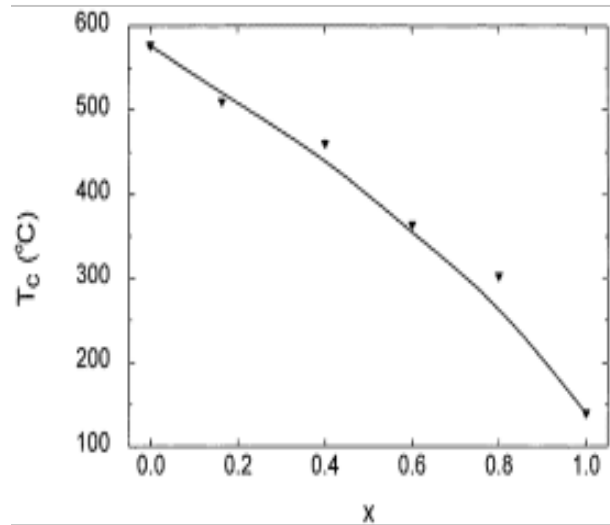
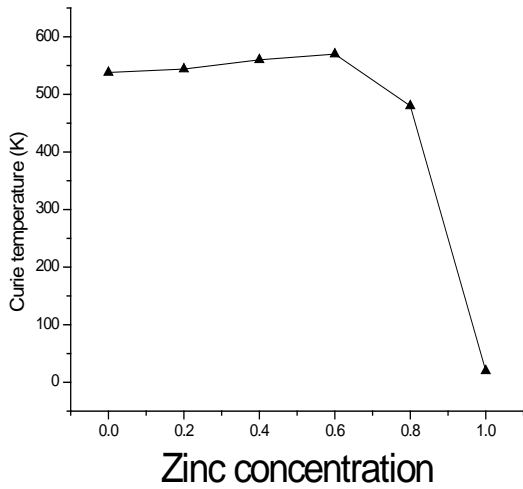
Table 2: The Variation of Magnetic Loss Factor ($\tan \mu_i$) with Additive Concentration

S.No.	Substituent conc. (x)	Magnetic loss factor	
		Sb	Zn
1	0.00	0.645	0.645
2	0.10	0.127	1.490
3	0.20	0.346	0.320
4	0.30	0.52	0.362
5	0.40	0.745	0.651
6	0.50	0.507	0.611

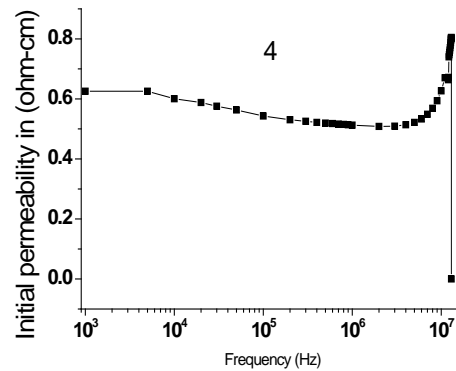
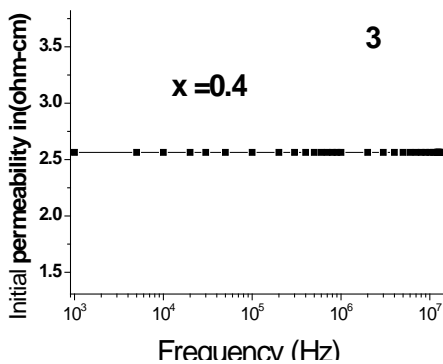
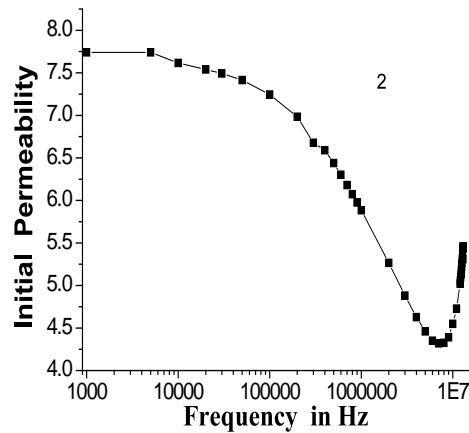
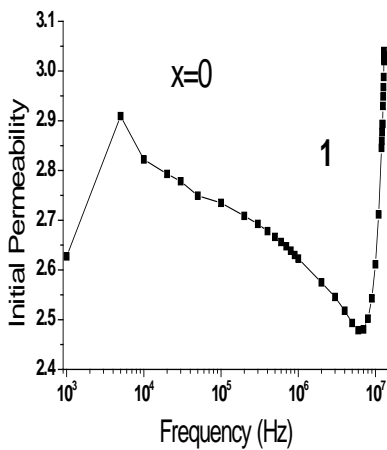
Table 3: The Relaxation Intensity ($\Delta\mu$) Real Part (μ^I) and Imaginary Part (μ^{II}) of Initial Permeability as a Function of Substituent Concentration

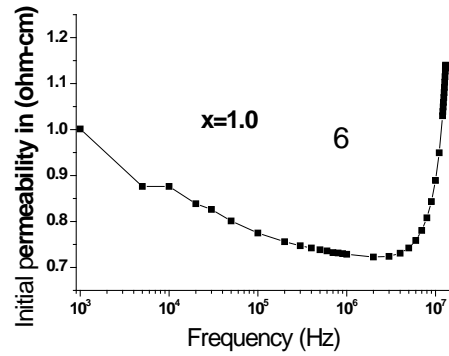
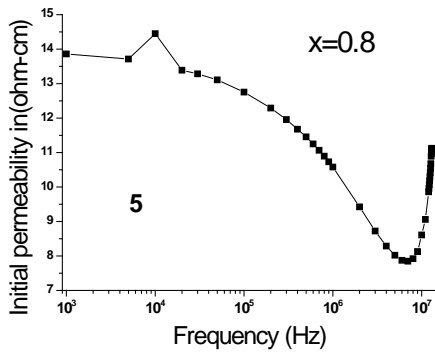
Substituent Conc. (x)	Antimony			Zinc		
	$\Delta\mu$	μ^I	μ^{II}	$\Delta\mu$	μ^I	μ^{II}
0.00	34.00	47.00	30.38	34.00	47.00	30.38
0.10	4.46	14.08	1.97	7.32	41.22	6.14
0.20	2.15	15.62	5.40	1.28	9.61	3.07
0.30	3.43	9.40	4.80	6.39	7.96	2.88
0.40	1.76	5.30	2.01	1.97	4.33	2.82
0.50	3.7	13.60	6.9	7.13	11.38	6.95

Plots of (1) Zn and (2) Sb: Variation Of Curie Temperature With Dopant Concentration ‘x’

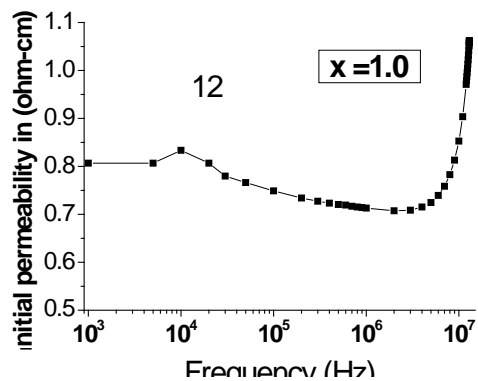
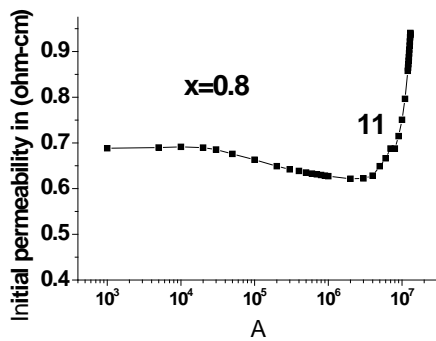
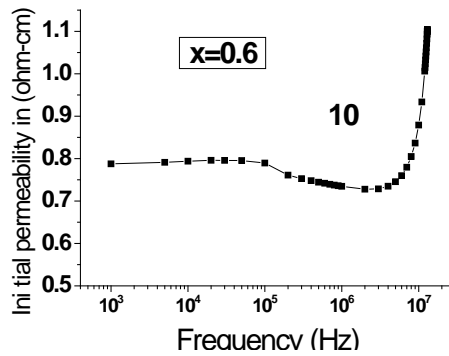
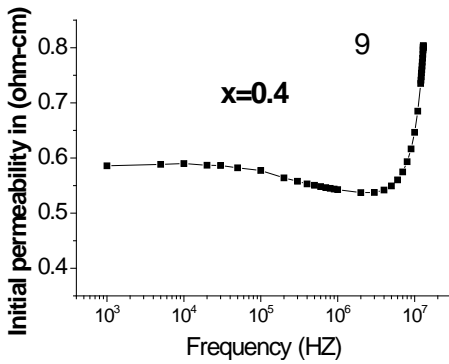
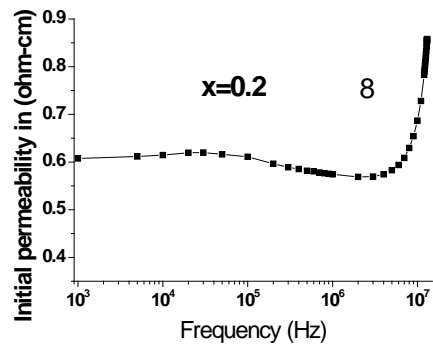
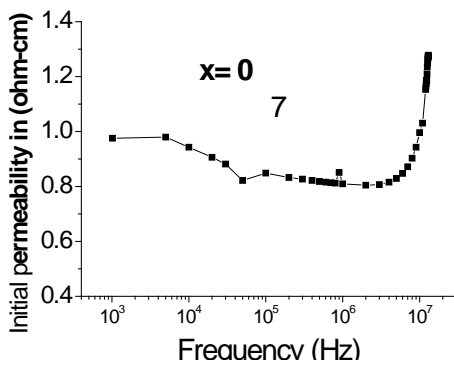


Plots of Frequency (Hz) Vs Initial Permeability (ohm-cm):(1 to 6, for Zn dopant)





Plots of Frequency(Hz) Vs Initial permeability(ohm-cm): (7 to 12, for Sb dopant)



Globus et al [51, 52] pointed out that domain wall bulging would still permit wall movement even while the end points were tied down. The domain walls bulge under application of magnetic field until a critical field H_{cr} causing the wall to get unpinned. According to this model the domain wall Energy per unit area (γ) is calculated using the formula. $\{(\mu_i - 1) = (3 Ms^2 Dg)/16 \gamma\}$, Where Ms is saturation magnetization, Dg is grain diameter, μ_i is the initial permeability.

The evaluated values using the formula are already communicated and available elsewhere [39]. The substitution of Sb^{5+} or Zn^{2+} is led to the increase of domain wall energy with substituent concentration up to $x = 0.20$. For further concentration it is found to decrease. Low concentration of substituent with the increased domain wall energy is suitable to induce driving force for the movement of grain boundary resulting increase in grain size. The decrease of γ at higher concentrations of substituents depicts its small contribution for grain growth because of the undetected impurity phase that formed.

If the formed grains are free from the pores and defects, then a plot of Dg versus μ_i , in general exhibits a linear relationship. Deviation from linearity due to microstructural effects reflects on the quality of the ferrite. μ_i , and Dg are found to follow linear relationship for Mo substituted ferrites while in the case of Sb added ferrites correlation between μ_i , and Dg is not observed.

Earlier for **Li-Zn** ferrites linear relationship between μ_i and Dg was observed by N. Rezlescu and E.Rezlescu [53] with the addition of Sb_2O_5 . This linearity was interpreted by the Globus model [52]. According to this model the relation between Dg and μ_i was explained based on bulging of domain walls that exist inside the grains.

Shun Hua Xiao et.al., [54] prepared Cobalt ferrite ($CoFe_2O_4$) Nano powder by a low-temperature, auto-combustion method and studied its thermal evolution of the precursor, the microstructure, morphology and magnetic properties. The report that the synthetic process was a thermally induced redox reaction with carboxyl group as reductant and NO_3^{-1} ions as oxidant. The grains observed in as-burnt powder were proved to be $CoFe_2O_4$ Nano crystallites with high dispersibility and low agglomeration. Both the saturation magnetization (M_s) and the remnant magnetization (M_r) were found to be highly depending upon the annealing temperature. The highest coercivity (1373 Oe) was achieved by the sample annealed at 400 °C & their results indicate that the method might provide a promising option for synthesizing high-quality $CoFe_2O_4$ Nano powder.

C N Chinnasamy et.al.[55] prepared Nanostructured $ZnFe_2O_4$ ferrites with different grain sizes by high energy

ball milling for various milling times. Both the average grain size and the root mean square strain were estimated from the x-ray diffraction line broadening. The lattice parameter initially decreased slightly with milling and increased with further milling. The magnetization is found to increase as the grain size decreased and its large value is attributed to the cation inversion associated with grain size reduction. The ^{57}Fe Mossbauer spectra were recorded at 300 K and 77 K for the samples with grain sizes of 22 and 11 nm. There was no evidence for the presence of the Fe^{2+} charge state. At 77 K the Mossbauer spectra consist of a magnetically ordered component along with a doublet due to the super paramagnetic behavior of small crystalline grains with the super paramagnetic component decreasing with grain size reduction. At 4.2 K the sample with 11 nm grain size displays a magnetically blocked state as revealed by the Mossbauer spectrum. The Mossbauer spectrum of this sample recorded at 10 K in an external magnetic field of 6 T applied parallel to the direction of gamma rays clearly shows ferri magnetic ordering of the sample. Also, the sample exhibits spin canting with a large canting angle, maybe due to a spin-glass-like surface layer or grain boundary anisotropies in the material. These findings of different authors conclude that $ZnFe_2O_4$ is ferrimagnetically ordered in nanocrystalline form irrespective of the method of preparation of the samples'.

ACKNOWLEDGEMENTS

R.Dhanaraju, sincerely thanks the U.G.C, for the award of research fellowship, with which the work reported in this communication could be done .The authors thank the Technical officer

Dr. S. Manjunathrao scientist in charge of Vibration Sample Magnetometer set up , and Dr. S. M. Ahmed, Principal Scientific officer from : Central Instruments Laboratory, Central University of Hyderabad, INDIA, for helping in the usage of the VSM and associated devices . They also thank Dr. K. Trinadh, Additional Director & Dr. N. S. Naidu, Scientist 'F', both of Naval Science and Technological Laboratories, DRDO, Ministry of Defence, Govt. of India Visakhapatnam-530027, A.P. INDIA for their help in using the techniques for dielectric and conductivity measurements.

REFERENCES

- [1] Alex Goldman(2006), "Modern Ferrite Technology", 2nd Edition, (ISBN10:0-387-29413-9)Springer Publication, <springeronline.com>
- [2] H.Hamdeh,et.al., (1997) 1.Appl.Phys , 81 , p1851

- [3] Murthy V R K et.al.,(1990) Ferrite Materials Science and Technology, Narosa Publishing House, New Delhi-IS 8
- [4] B.D.Cullity, (1972) Introduction to magnetic materials, Addison Wesley publishing Company 159
- [5] Soshin Chikazumi, (1964)Physics of magnetism, John Wiley and sons, Inc., New
- [6] Ronald F.Sooahoo, (1960) ,Theory and application of ferrites, Prentice hall Inc, New Jersey 46
- [7] Magnetic Instrumentation Technote 97- 01, www.kjstmagnetics.com/tech.htm
- [8] S.R.Trout et.al., (2002), 'Magnetic testing of Bonded magnets' ,For the NATO/ARW Conference on Bonded Magnets, August 22 and 23, 2002, Newark, DE, U.S.A.,
- [9] R..Dhanaraju et.al. (2011), "Measurements of Electrical characteristics of Zn & Sb substituted Cu ferrites, and the frequency dependence of resistivity for Zn substituted Cu ferrite" in 'SCIENCE & SOCIETY', (ISSN 0973-0206), Proc. Of. Nat. Sym.on Nano.Sci.and Tech-2011.9(2), pp 97-102.
- [10] R. Dhanaraju et.al.,(2011), 'SEM and XRD studies on Sb substituted Cu ferrite nanomaterial' In 'SCIENCE & SOCIETY' (ISSN 0973-0206), Proc.Of.Nat.Sym.on Nano.Sci.and Tech-2011.9(2), pp 103-108
- [11] R.Dhanaraju et.al. (2011), 'Graphical traits about VHTM in the light of FTIR Studies on Zn & Sb substituted Cu ferrites' , International Journal of Engineering Science and Technology, 3 (11), pp 8058-8064
- [12] R.Dhanaraju et.al. (2012), 'Verwey's Hopping Transition Mechanism in relation to Dielectric studies of Zn & Sb substituted Cu ferrites'. ,communicated to The International Journal of Science & Technology (ISSN 2049-7318), Submission Reference : IJST_23221113388215
- [13] Simon Foner,(1959) "Versatile and Sensitive Vibrating Sample Magnetometer," Review of Scientific Instruments, 30 (1959) pp. 548-557
- [14] J.Smit, and H.P.J. Wijn, (1959) Ferrites, Philips Technical Library, 33 York 9
- [15] S.R.Trout (2002), 'Magnetic Testing of Bonded Magnets' For the NATO/ARW Conference on Bonded Magnets, August 22 and 23, 2002, Newark, DE, USA
- [16] Curie, P. (1895) Ann. chim phys.[7] 5, 289
- [17] Neel, L. (1932) Ann. de Phys. 17, 6 ;
- [18] Rath, C., et.al.,(2000), Applied Physics Letters, Vol. 76, No.4 p. 475-7.
- [19] Alex Goldman (2006), Chapter-18, 'Magnetic Measurements', p404-406, "Modern Ferrite Technology", 2nd Edition, (ISBN10:0-387-29413-9), Springer Publication, <springeronline.com>
- [20] Rathenau G.W.AND Snoek J.L,(1946), Philips Res Rept1, p239
- [21] D.J. Perduijn et.al. (1968) , Proc. Brit. Ceram. Soc., 10 , p 263.
- [22] Ing Carl Beck, (1974), 'Magnetic material and their applications', Butterworth's, London,
- [23] V. Sepelak, et.al., (1997), "Structure and properties of the ball-milled spinel ferrites," Materials Science and Engineering A, vol. 22, pp. 226–228,
- [24] S. A. Oliver, et.al., (2000), "Large zinc cation occupancy of octahedral sites in mechanically activated zinc ferrite powders," Applied Physics Letters, vol. 76, no. 19, pp. 2761–2763,
- [25] B. Jeyadevan, et.al., (1994), "Structure analysis of coprecipitated ZnFe₂O₄ by extended x-ray-absorption fine structure," Journal of Applied Physics, vol. 76, no. 10, pp. 6325–6327,
- [26] C. N. Chinnasamy, et.al., (2000), "Magnetic properties of nanostructured ferrimagnetic zinc ferrite," Journal of Physics Condensed Matter, vol. 12, no. 35, pp. 7795–7805,
- [27] F. S. Li, et.al., (2004), "Site preference of Fe in nanoparticles of ZnFe₂O₄," Journal of Magnetism and Magnetic Materials, vol. 268, no. 3, pp. 332–339,
- [28] L. D. Tung, et.al., (2002) , "Annealing effects on the magnetic properties of Nano crystalline zinc ferrite," Journal of Magnetism and Magnetic Materials, vol. 319, no. 1–4, pp. 116–121,

- [29] C. Upadhyay, et.al., (2007), "Effect of size and synthesis route on the magnetic properties of chemically prepared Nano size ZnFe₂O₄," Journal of Magnetism and Magnetic Materials, vol. 312, no. 2, pp. 271–279,
- [30] H. Xue, et.al., (2007), "Facile synthesis of Nano crystalline zinc ferrite via a self-propagating combustion method," Materials Letters, vol. 61, no. 2, pp. 347–350,
- [31] M. Atif, et.al. (2006), "Magnetization of sol-gel prepared zinc ferrite nanoparticles: Effects of inversion and particle size," Solid State Communications, vol. 138, no. 8, pp. 416–421,
- [32] C. Yao, et.al., (2007), "ZnFe₂O₄ Nano crystals: synthesis and magnetic properties," Journal of Physical Chemistry C, vol. 111, no. 33, pp. 12274–12278,
- [33] S. Nakashima, et.al.,(2005), "High magnetization and the high-temperature super paramagnetic transition with intercluster interaction in disordered zinc ferrite thin film," Journal of Physics Condensed Matter, vol. 17, no. 1, pp. 137–149,
- [34] J. Chen, et.al., (1995), "Observation of super Para magnetism in rf-sputtered films of zinc ferrite," Journal of Magnetism and Magnetic Materials, vol. 146, no. 3, pp. 291–297,
- [35] R. Nawathey, et.al., (1989) , "Pulsed laser-induced vaporization from the surface of a binary oxide (zinc ferrite) and its implications for synthesis of thin films," Journal of Applied Physics, vol. 65, no. 8, pp. 3197–3204,
- [36] M. Taheri, et.al.,(2002) , "Magnetism and structure of Zn_xFe_{3-x}O₄ films processed via spin-spray deposition," Journal of Applied Physics, vol. 91, no. 10, Article ID 7595, 3 pages,
- [37] M. Bohra, et.al., (2006), "Large room temperature magnetization in Nano crystalline zinc ferrite thin films," Applied Physics Letters, vol. 88, no. 26, Article ID 262506,
- [38] Yan Xu et.al.,(2010), 'Preparation and Magnetic Properties of ZnFe₂O₄ Nanotubes', J.Nanomaterials Volume 2011, Article ID 525967, 5 pages
- [39] R.Dhanaraju et.al.,(2012), 'Hysteresis and related magnetic studies on Zn & Sb substituted Cu ferrites in relation to Verwey's Hopping Transition Mechanism', communicated to International Journal of Science & Technology (ISSN 2049-7318) on 24th Feb 2012, ,Manuscript reference number IJST_6999413389535
- [40] S.R. Sawant et.al., (1981) , [Solid State Communications, 40\(4\),pp 391-394,](#)
- [41] H. Ehrhardt, et.al., (2003), "Magnetism of the nanostructured spinel zinc ferrite," Scripta Materialia, vol.48, no. 8, pp. 1141–1146,
- [42] S. Bid et.al., (2003) ,"Preparation of zinc ferrite by highenergy ball-milling and microstructure characterization by Rietveld's analysis," Materials Chemistry and Physics, vol. 82, no. 1, pp. 27–37,
- [43] A. Kundu, et.al., (2003) ,"Magnetic properties of a partially inverted zinc ferrite synthesized by a new coprecipitation technique using urea," Physics Letters A, vol. 311, no. 4-5, pp. 410–415.,
- [44] S. Chikazum (1964) , 'Physics of Magnetics' John Wiley and sons Inc. New (1964) 263.
- [45] J.J. Went et.al.,(1951), Phys. Rev., 82 (1951) 269.
- [46] Neel,L. (1948), Ann. de Phys. (12) 3, 137
- [47] L.A. Vladimirtseva et.al.,(1973), Sov. Powder Metall. & Met.Ceram. (USA), 12 (1973) 669.
- [48] K. Ramanathan et.al., (1971) IEEE Trans. On Mag., MAG-7 (1971) 613.
- [49] L.G. Van Uitert,(1955), J.Appl. Phys., 26 (1955) 1289
- [50] M.Kolenbrander and P.J. Van der Zaag (1997), J. Phys IV France 7 (1997) C1-195.
- [51] Globus. A and Guyot.(1972), M. Stat. Solid 52 (1972) 427.
- [52] Globus, J (1977) ,de PHYS 38 (1977) CI-1 (Proc. 3rd Int. Ferrites conf.)
- [53] N. Rezlescu and E.Rezlescu, (1996), J.of Am. Ceram. Soc., 79[8] ,p2105.
- [54] Shun Hua Xiao et.al., (2007) ,'Low-temperature auto-combustion synthesis and magnetic properties of cobalt ferrite nanopowder',in [Materials Chemistry and Physics, 106\(1\)](#), PP82-87

[55] C N Chinnasamy et.al., (2000), 'Magnetic properties of nanostructured ferrimagnetic zinc ferrite' , J. Phys.: Condens. Matter,12(35) p7795; Ibid , C N Chinnasamy et al.,(2001) ,J. Phys.: Condens. Matter 13 1179

[56] R.Dhanaraju et.al.,(2012), 'Hysteresis and related magnetic studies on Zn & Sb substituted Cu ferrites in relation to Verwey's Hopping Transition Mechanism', communicated to The International Journal of Science & Technology (ISSN 2049-7318), , Submission Reference : IJST_6999413389535